



Graphene and graphene oxide based aerogels: Synthesis, characteristics and supercapacitor applications



Satiye Korkmaz^a, İ. Afşin Kariper^{b,c,*}

^a Karabük University, Engineering Faculty, Karabük, Turkey

^b Erciyes University, Education Faculty, Kayseri, Turkey

^c Erciyes Teknopark, Building 1, No:41, Kayseri, Turkey

ARTICLE INFO

Keywords:

Graphene oxide
Aerogel
Graphene oxide aerogel
Supercapacitor

ABSTRACT

Graphene and graphene-based materials have a high potential, especially in energy storage technology. Thanks to the three-dimensional (3D) structures developed with this material, their importance in the production and application of energy storage devices has increased. Studies on supercapacitor applications of graphene-based aerogels have begun to arouse interest in recent years. In this study, recent studies on aerogel supercapacitors, in which researchers have shown great interest, have been compiled and collected. In this study, production methods and properties of graphene oxide, properties and production of aerogels, production and applications of graphene/graphene oxide aerogels are discussed. In this way, the data is presented and discussed in an organized way for the researchers who study or who want to study in this field.

1. Introduction

Today's rapidly depleted energy resources and the deteriorating ecological balance prioritized the need for energy storage systems. Moreover, the growing popularity of telecommunications equipment, backup storage devices, portable electronic devices, cardiac pacemakers and hybrid electric vehicles has aroused great interest towards energy storage devices. In this context, supercapacitors, which are mostly preferred among various energy storage devices, are electrochemical energy storage devices that cover the gap between batteries and dielectric capacitors with their high-power density, high specific energy and long life (>100,000 cycles) [1]. Furthermore, flexible solid-state supercapacitors are important for wearable electronic devices [2], [3].

Graphene, which come into prominence with wide specific surface area (SSA) ($2630 \text{ m}^2\text{g}^{-1}$), high electrical conductivity and chemical stability, as well as excellent mechanical, thermal and optical properties, has become popular especially for supercapacitors. However, a serious loss in surface area is observed due to the re-stacking of graphene layers during chemical reduction. The conversion of graphene nanotubes to graphene aerogel having a stable three-dimensional network solves this problem. The re-stacking problem resulting from π - π interactions between graphene layers and the Van der Waals forces are solved and the layers are chemically bonded together. Thus, the structure is intended to provide better performance in supercapacitors

with much higher electronic conductivity, rapid charge transport between the layers and the resulting high surface area. The most interesting feature of GOs is that they are well protected by a hexagonal structure having functional groups such as hydroxyl, epoxide, carboxyl and some randomly distributed alkyl groups in the plane, together with a clear AB stacking order. Hydroxyl and epoxide functional groups are located close to each other in the basal planes, whereas carboxyl and alkyl groups are located at the edges of GO flakes. With longer oxidation times, hydroxyl groups are converted to more epoxide groups in the basal plane. Our discovery of the GOs graphite structure with AB stacking order will provide positive contributions in potential graphene applications [4]. However, GO has poor electrical conductivity, so there is a need for reduction. There are several reduction methods developed to increase the electrical conductivity of GO, however, an additional problem arises after the reduction process. Therefore, it is important to make the graphite or graphene itself water soluble. For versatile applications, well-dispersed graphene in water-based solution can be coated onto any substrate by spraying or rotating, which makes it easier to produce composites or more derivatives via chemical synthesis [5]. In addition, graphene/conductive polymer, graphene/metal oxide composites improved the low conductivity and unstable structures of polymers and metal oxides thanks to high electrical conductivity of graphene. Supercapacitors have limited commercial applications due to their low energy density and high cost. Up to today, graphene aerogel-based materials has aroused great interest because of their low-cost,

* Corresponding author at: Erciyes University, Erciyes Univ., Faculty of Education, 38039 Kayseri, Kayseri, Turkey.

E-mail addresses: akariper@gmail.com, akariper@erciyes.edu.tr (İ.A. Kariper).

large surface area, high electrical conductivity and good chemical stability. Some strategies have been developed to improve the existing specific capacitance of graphene aerogel-based materials. First of them is graphene aerogels formed by adding graphene oxides into various alcohols in order to increase the porous nanostructures, mechanical property and conductivity [4]. The second one is the hybrid structures obtained by inserting Co (OH), Co₃O₄, MnO₂, MoO₃, MoS₂ [5–10] materials into the graphene aerogel. Researches have shown that inserting these materials into the structure plays an important role in increasing the capacitance of graphene aerogel-based supercapacitors. Another strategy is to functionalize graphene aerogels with oxygen, nitrogen, sulfur, boron or sulfur. Studies have shown that nitrogen, which forms strong atomic bonds due to atomic size similar to carbon atoms, can easily be doped into graphite structure and nitrogen contribution on graphite surface increases charge transfer rate. Nitrogen doped graphite has been a promising approach for better performance of metal-free carbon-based capacitors having better chemical reactivity than pure graphite [13]. The aforementioned functional groups contribute to the increase of the capacitance with the electronic and ionic transfer between the surface of the electrode material and the electrolyte in the supercapacitors. In this way, the band structures therefore the electronic structures of the graphene can be altered by the use of heteroatom functional groups, which improves their specific capacitance [11–13].

The combination of carbon materials (such as CNTs and graphene) and metal oxides (RuO₂, NiO, Co₃O₄, MnO₂) allows the specific capacitance to increase [14–19]. On the other hand, carbon aerogels exhibit higher electrical conductivity due to their three-dimensional network. Moreover, in order to overcome limited power density and energy capacity, both surface area and pore volume are increased by the activation of KOH and CO₂. CNT aerogels are a good alternative for supercapacitors with their high specific surface area, electrical conductivity, low density and excellent mechanical properties.

2. Graphene Oxide

Graphene is an exciting material with its specific surface area (2630 m²g⁻¹), high young modulus (~ 1 TPa), thermal conductivity (~ 5000 Wm⁻¹K⁻¹) and optical transmittance (~ 97,7%) and good electrical conductivity.

Graphene is a carbon allotrope in the form of a two-dimensional and atomic-sized hexagonal lattice. Fullerenes and CNTs are the basic building unit of all graphite carbons. Graphite layers can be synthesized by different methods such as mechanical cleavage of graphite, chemical decomposition of graphite, dissolution of carbon nanotubes, epitaxial growth on SiC surface and chemical vapor deposition. Among these synthesis methods, it is possible to produce the highest quality graphene via mechanical cleavage and to increase the productivity of graphene by chemical method.

Graphene differs from AC and CNTs. The illustration in Fig. 1 shows that graphene is characterized by a unique morphology described by a monolayer 2-D lattice structure of carbon atoms, thus, the accessible surface area of the graphene is different from other carbon materials used in the EDLCs. While other materials rely on a fixed porous structure for the transport and adsorption of electrolyte ions, a well-distributed graphene layer in a solution provides a theoretical surface area of 2630 m²g⁻¹.

Although the surface area of the graphene oxide is less than that of graphene, graphene oxide exhibited a high capacitance, probably due to the oxygen-containing functional groups on the surface (in Fig. 2).

Graphene oxide showed better cycle stability compared to graphene. Because of good performance and low cost, graphene oxide is considered to be a better option than graphene as electrode material in supercapacitors [20]. Due to its high conductivity and mechanical stability, graphene is also suitable for use as a substrate for active materials such as faradaic materials with pseudo capacity. Although,

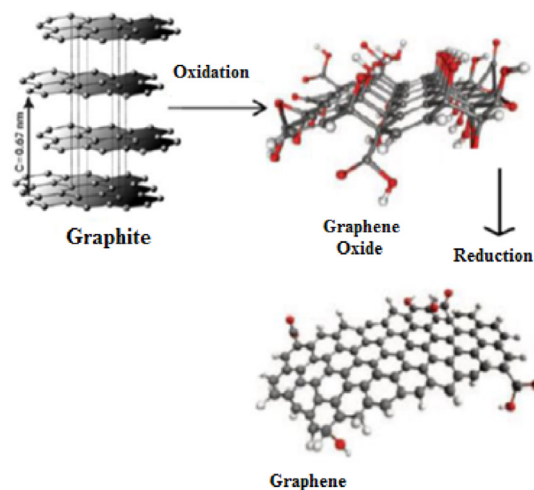


Fig. 1. Synthesis of chemically derived graphene.

high energy density and power density are difficult to obtain with pure carbon materials for supercapacitors, they still play an important role in obtaining high performance supercapacitors because of their high surface area and superior conductivity. Currently, the strategy for developing supercapacitors with high power density and energy density is coating carbon materials homogeneously with a thin sheet of faradaic material. With the help of conductive carbon materials having high surface area, the active materials can apply high pseudo capacitance and may highly contribute to the energy density.

Graphene oxide (GO) has been synthesized since the early 19th century by the methods of Brodie, Staundenmaier, Offeman and Hummers. These methods are based on the oxidation of graphite with strong acid and oxidants. The degree of oxidation varies according to the method used, the conditions of the reaction and the properties of the graphite. However, toxic chemicals are used in graphene oxide (GO) production methods and toxic gas is produced during the process. In the Hummers method, graphite is reacted with strong oxidizing agents such as potassium permanganate and high concentration of sulfuric acid [22]. Epoxy and hydroxyl functional groups are embedded into the graphite structure after oxidation in Hummers method. Functional groups containing water and oxygen are drawn into the layers through mixing process, a strong interaction is accomplished, and the layers are removed from each other. By this way, the graphite, which is hydrophobic, is transformed into a hydrophilic and dispersed GO [20]. The usage areas of GO are expanding day by day because of easy dissolution in solvents, its dielectric property, its transparency, its adjustable electronic properties and its superior mechanical properties. On the other hand, GO with hydrophilic property becomes insulating in terms of electrical conductivity due to spoilage of sp² bonds [20]. Furthermore, the reaction of GO with reductants yields reduced graphene oxide (RGO) with hydrophobic properties [21–23]. Reductants such as hydrazine, dimethyl hydrazine, hydroquinone, sodium borohydride (NaBH₄), ascorbic acid, amino acid, sodium hydroxide (NaOH), hydroiodic acid, vitamin C, sodium bisulfite (NaHSO₃) are used in the reduction process [21,24,25]. The characteristics of GO are very important for achieving the desired properties of RGO [21–23].

3. Aerogels

As is known, the matter is present in three forms as solid, liquid and gas. As shown in Fig. 3, the densities of the solid and liquid or gas and plasma are the same. Accordingly, it would not be wrong to see aerogel as a new state of matter [24]. Aerogels are the lightest solid materials known with their low density (0.003–0.15 kgm⁻³), high porosity and large surface areas (500–1000 m²g⁻¹). Nowadays, aerogels, which are mostly preferred for thermal insulation, attract attention with the high

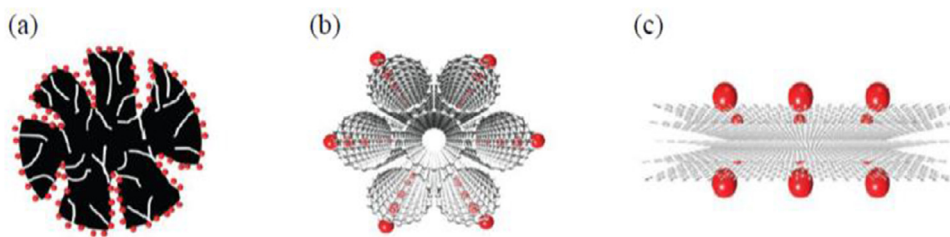


Fig. 2. Comparison of carbon materials in terms of usability as EC electrodes: a) Activated Carbon, b) Carbon Nanotube, c) Graphene.

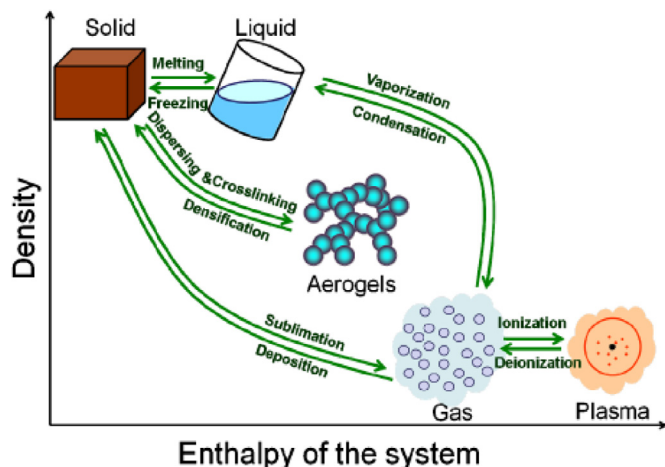


Fig. 3. The distribution of the states and density of different matters “Enthalpy of the system” diagrams.

performance that they exhibited in recent years in supercapacitors, in addition to be used in filling materials and tissue engineering,

Aerogels have good mechanical and physicochemical properties as well as adjustable pore sizes and surface areas. In particular, since the aforementioned properties of hybrid aerogels can be changed, it is thought that new aerogel varieties can be developed in the coming years. The gel can be formed in different forms since it can be shaped during gel formation. Organic and carbon aerogels are commercially available in small quantities to be used in academic studies. In addition, some academics are able to commercialize the aerogels they develop. This suggests that aerogels have a high growth potential [26].

Aerogel production consists of three stages: gel formation, solvent exchange and drying process. The shape of the aerogel (granule, powder) is determined during gel formation. This step will also allow the determination of the microstructure of the aerogel to be obtained. Solvent exchange and drying processes are important to keep the shape of the aerogel. In fact, the drying process can be carried out in supercritical conditions or at low pressure and at a temperature below the melting point (freeze-drying). In general, the most reliable and environmentally friendly drying method used is supercritical drying. The freeze-drying process is also an alternative, but it requires a long process (tens of hours) [26].

The cost and availability of the raw materials used in production play an important role in the diversification of aerogels. In the production of silica aerogels, ash of various (industrial) bio-wastes containing silica species such as rice husk, oil cake, oil chyle, fly and wheat husk are used. Biopolymers (alginate, pectin, chitosan and proteins) are used in the production of organic aerogels and they also serve as a source for carbon aerogels. On the other hand, recyclable materials (such as paper or plastic) play an important role in the production of organic aerogels. In the academic studies, a large number of organic aerogels have been studied and European Union projects have been developed, but studies on inorganic aerogels are limited.

There are some basic gaps and deficiencies related to aerogels. In

this context, to understand and develop hybrid aerogels, it is important to investigate their structure-property relationships by examining the individual characteristics of each polymer forming the aerogel. Furthermore, in order to make more accurate comparisons, the characterization of aerogels should be standardized and catalogs should be prepared [26].

Synthetic polymers and biopolymers are of great interest in the production of aerogels. Biopolymers obtained from various sources such as polysaccharides (alginate, cellulose, pectin, chitosan, chitin), lignin, and proteins are used as precursors. Since the final aerogels will carry the characteristics of the starting raw materials, the functions of biopolymer aerogels can be improved by working on the properties of the raw materials used.

Hybrid aerogels, which are obtained from the combination of different polymers with inorganic materials and the completion with a third material, have a high potential. In addition, after drying a coating process can be performed, which allows the function of the aerogel to be extended.

Another noteworthy group of aerogels is conductive aerogels. Regarding the aerogels obtained by a variety of carbon-based aerogels and their combinations such as carbon nanotubes, graphene and graphene oxide, the initial gel structure allows the determination of the structure of the final aerogel (such as the pore size) in advance. It also provides the opportunity to increase the conductivity of the aerogel by doping or coating. This will improve the application potential of conductive aerogels, especially in supercapacitors.

3.1. Classification and production of aerogels

As shown in Fig. 4, aerogels can be examined in two categories as single-component and composite aerogels. Single-component aerogels contain; oxide (silica and non-silica), organic (resin and cellulose based), carbon (carbonized plastic, CNT and graphene), chalcogenide and other aerogels (single element, carbide). Whereas composite

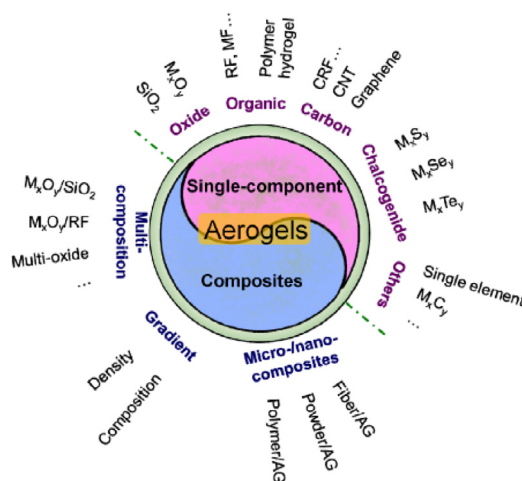


Fig. 4. Classification of aerogels.



Fig. 5. Basic research scheme for aerogel.

aerogels can be classified as; multicomponent, gradient and micro / nano aerogel [25].

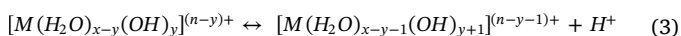
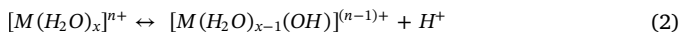
Generally, aerogel preparation process takes place in three steps. As shown in Fig. 5, the particles on the left are spontaneously formed in the precursor solution and catalyzed by the catalysts through hydrolysis and condensation reactions. The particles on the left are then cross-linked and combined with a compatible gel. The solvent in the gel is dried before the microstructure damage occurs. Various drying methods include; drying at supercritical temperature, low-temperature drying, natural drying, solvent-modified ambient drying, surface modified drying and freeze-drying methods [[27], [28]].

One of the production methods for oxide-based aerogels is the traditional sol-gel (TS) method. As shown in Fig. 6, the metal alkoxide alkoxy group reacts to form the hydroxyl group. Condensation occurs when the alkoxide is partially hydrolyzed, a dehydration reaction occurs between different metal atoms or the hydroxyl group and the alkoxy group are bridged with an oxygen atom.

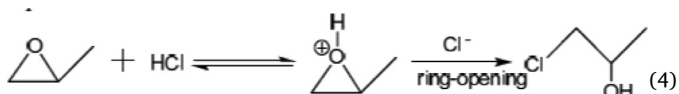
In the epoxide addition (EA) method developed by Gash, salt and epoxide were used as precursors. The epoxide reacts more slowly with hydrogen ion under acidic conditions to facilitate condensation. The epoxide addition (EA) method consists of three processes, namely hydration, hydrolysis and condensation. As shown in formula (1), the metal salt in a water-containing solution is present in the form of hydrated ion (by the hydration reaction).



The multi-stage hydrolysis reactions of the hydrated ion spontaneously occur as shown in formulas (2) and (3). The reaction produces hydrogen ion and makes the solution partially acidic.



The epoxide cannot rapidly increase the pH value as an alkali, but gradually uses hydrogen ion via a ring-opening nucleophilic addition reaction (formula (4), for example propylene oxide and hydrochloric acid). Therefore, the balance of hydrolysis turns to the right and after the epoxide is added, it produces ions with hydroxyl.



Thereafter, dehydration condensation occurs by attaching different hydroxylated ions to an oxygen bridge. Condensation is rapid, but it is limited to a low ratio of epoxide catalyzed hydrolysis. Furthermore, the epoxide keeps the initial condition acidic and facilitates slight

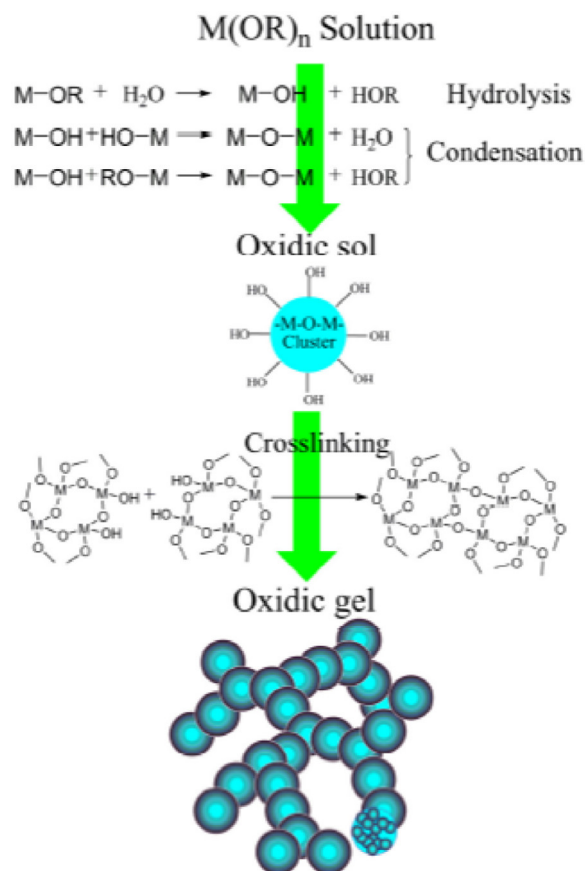
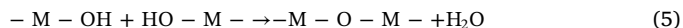


Fig. 6. The general scheme of the traditional sol-gel method.

condensation compared to the alkaline condition. Both effects reduce the rate of condensation.



The left particles are then formed, crosslinked and combined with a gel, similar to the process described in the TS method. The epoxide can lead to a relatively low hydrolysis and condensation rate (particularly condensation rate), because the solution system may remain in a low pH environment for a long time. Iron oxide aerogels [[29],[30]], nickel-based aerogels [[31], [32]], alumina aerogels [33], stannic oxide aerogels [34], chromium aerogels [35], [36], tantalum oxide aerogels etc. [37–39] are prepared by EA method. In addition, this method was then used to prepare monolithic oxidic gels with various major elements such as Li (I), Al (III), Ca (II), Ti (IV), Cr (III), Mn (II), Fe (III), Co (II), Ni (II), Cu (II), Zn (II), Zr (IV), Mo (IV), Cd (II) and Ta (IV).

DIS (dispersed inorganic sol-gel) method has wide applicability in aerogel preparation technology, because in almost all trials the same process and parameters, even the same mixing ratio are used [36]. The polyacrylic acid can increase the rate of nucleation due to activation of the carboxyl region and reduce the rate of growth by decreasing the residual-ion concentration after rapid nucleation. Therefore, the reactivity differences between different elements are further reduced. PAA, which acts as both a dispersor and a template, distributes the colloid system and directs gel formation. In addition, carboxyl provides extra cross-linking and limits the formation of the terminal group, which can increase the formation of the gel. However, the DIS method is a newly developed method that needs more work.

Almost all kinds of stable metal-oxide aerogels can be easily prepared by DIS or EA method. On the other hand, the acid-catalyzed RF sol (developed by Leventis et al.) is easy to intertwine with metal oxide networks together with a suitable solvent. In this way, potentially more types of carbide aerogels or single element aerogels can be prepared by

magnesia thermic reduction.

Carbonized RF aerogel is considered to be one of the highly efficient electrode materials for supercapacitor or capacitive deionization. Chien et al. using nickel-cobalt/carbon aerogel as electrode recently reported that it is an excellent supercapacitor with ultra-high specific capacitance ($\sim 1700 \text{ F g}^{-1}$, which is much higher than the value of a single carbon aerogel $\sim 200 \text{ F g}^{-1}$), high rate capability and exceptional cycle stability [40]. Therefore, the use of metal oxide/CRF (RF = resorcinol formaldehyde) composite aerogels is a good way to improve capacitive properties [[41], [42]]. In addition, the aerogel is versatile for high-energy physics experiments. For example, ultra-light metal oxide/silica aerogels can greatly increase the efficiency of laser-X-ray transformation [43–50].

Carbon aerogels, invented by Pekala and colleagues, have some unique features that are preferred by a range of technologies, such as energy storage, catalysis, filtration and actuators [51]. First, carbon is a fairly light element, so the materials made from it have the potential to be very low density. Moreover, carbon-based aerogels can also be designed to have ultra-high surface areas. Carbon-based aerogels provide electrical conductivity and mechanical properties which are better than equivalent concentrations of inorganic aerogels. Inorganic aerogels will crumble when bent or will disintegrate with an irregular crash in the form of very low-density aerogels. In addition, low density ($<0.1 \text{ g cm}^{-3}$) inorganic aerogels are both excellent thermal insulators and excellent dielectric materials. Most carbon aerogels are both thermally and electrically good conductors. Therefore, materials with versatile features and capabilities can be produced by adjusting processing parameters and discovering new compositions [54]. Known carbon allotropes include not only CNT and graphene aerogels, but also diamond aerogels. CNT and graphene aerogels have shown a significant increase in the transport and mechanical properties compared to conventional carbon aerogels. In fact, because of the extraordinary properties of graphene aerogels, research on these materials has dramatically increased since the first report in 2009.

The excellent properties of carbon aerogels depend on the three-dimensional mesoporous characteristics of carbon nanoparticles. In general, carbon aerogels are produced by pyrolysis of resorcinol and formaldehyde-based organic aerogels via a sol-gel process. Micro coefficients of aerogels, in particular particle size and pore distribution, can be determined by different synthesis parameters, such as selection of reaction conditions, activation procedure, pyrolysis temperature and the presence of selected dopants.

4. Supercapacitor and Energy Storage

Supercapacitors are formed from two electrodes, an electrolyte, and a separator (Fig. 6). Like conventional capacitors, supercapacitors store the charge electrostatically or in the Farad, and no charge transfer is made between the electrode and the electrolyte. The charge accumulates on the electrode surfaces when voltage is applied. Following the natural attraction of different charges, the ions in the electrolyte solution are dispersed through the separator into the pores of the opposite charging electrode. However, electrodes are designed to prevent recombination of ions. This results in a two-layer charge on each electrode. These two layers, combined with an increase in surface area and a reduction in the distance between the electrodes, allow supercapacitors to achieve a higher energy density than conventional capacitors [55,56]. Since there is no charge transfer between the electrolyte and the electrode, there are no chemical changes associated with non-faradic processes. Therefore, the charge storage in the supercapacitors is recyclable, resulting in very high cyclic stability in (Fig. 7).

The components of a supercapacitor can be described as follows:

Ø **Electrode:** The capacitance value is proportional to the surface area of the electrode. Generally, carbon-based materials are used as the electrode material. The porous structure of the material allows more

charge carriers (electrolyte ions or radicals) to be stored in a given volume, which increases the capacitance of the supercapacitors. The electrodes are coated to the current collector and immersed into the electrolyte.

Ø **Electrolyte:** It is a key factor in determining internal resistance (ESR). Electrolyte solution may be aqueous or non-aqueous. Non-aqueous electrolytes are often preferred because they provide high output voltage (V). Non-aqueous solution consists of conductive salts dissolved in solvents. Acetonitrile or propylene carbonate are the most preferred solvents. Tetraalkylammonium or lithium ions can be used as solubilizing agents.

Ø **Separator:** It is placed between electrodes and made of material which is transparent for the ions and insulator for direct contact between porous electrodes to prevent short circuit.

The administration of the voltage to a supercapacitor leads to the development of an electric field with charging. When the voltage is applied, each collector draws opposite charged ions and electrolyte ions are accumulated on the surface of the two collectors.

As we can see in Fig. 8, as two separate charge layers are formed, the supercapacitor is also called the Electric Double Layer Capacitor (EDLC).

Referring to Fig. 8, in the discharge process in Fig. 9, the ions are not affected by current collectors and they are dispersed through the electrolyte. Thus, the discharge state begins to occur in both collectors.

5. Supercapacitor applications of graphene and graphene oxide based aerogels

Graphene and graphene-based materials have a high potential especially in energy storage technology. Thanks to the three-dimensional (3D) structures developed with this material, the production of energy storage devices and their importance in the applications has increased. Studies on supercapacitor applications of graphene-based aerogels have begun to arouse interest in recent years.

Song, Z. et al. synthesized the composite of nano-iron oxide (Fe_2O_3) / three-dimensional graphene aerogel ($\text{Fe}_2\text{O}_3/\text{GA}$) by a hydrothermal method. In the study, Fe_2O_3 particles were homogeneously encapsulated in graphene aerogel (GA). Electrochemical performance of $\text{Fe}_2\text{O}_3/\text{GA}$ was examined via cyclic voltammetry (CV) and galvanostatic load/discharge tests. In a three-electrode system, in 0.5 M Na_2SO_4 aqueous solution, a specific capacitance of 81.3 F g^{-1} was obtained at constant 1 Ag^{-1} current density, in the operating potential range from -0.8 to 0.8 V [52].

Chen, T.T. et al. obtained the three-dimensional (3D) graphene/porous carbon (LGN/PC) aerogel produced in two steps using the hydrothermal method (in Fig. 10). The highest capacity was measured up to 410 F g^{-1} at 0.1 Ag^{-1} , in the measurement performed in a system with three electrodes in 6 M KOH aqueous electrolyte. The solid-state supercapacitor based on 3D LGN / PC showed no significant loss of capacity after 5000 cycles at 5 Ag^{-1} current density [53].

Liu, Y. et al. first produced triple composites for aerogel-based asymmetrical supercapacitors. They combined rod-like MnO_2 and MnCO_3 hybrid nanostructures in particle form with graphene oxide for producing $\text{MnO}_2/\text{MnCO}_3/\text{rGO}$ aerogels (MGA), which have high electrical conductivity and mechanical strength (in Fig. 11). They were found to exhibit an energy density of 17.8 Wh kg^{-1} , in a potential range of $0-1.6 \text{ V}$ at 400 W kg^{-1} power density [54].

Lee, E.I. et al., have prepared a number of modified activated carbon aerogels to improve the electrochemical performance of activated carbon aerogel (ACA). For this purpose, they activated carbon aerogels with CO_2 using sol-gel (RF) method (in Fig. 12). For comparison, activated carbon aerogel (ACA) without HNO_3 oxidation was also analyzed. This study demonstrated that the surface oxygen group plays an important role in determining the electrochemical performance of modified activated carbon aerogels [55].

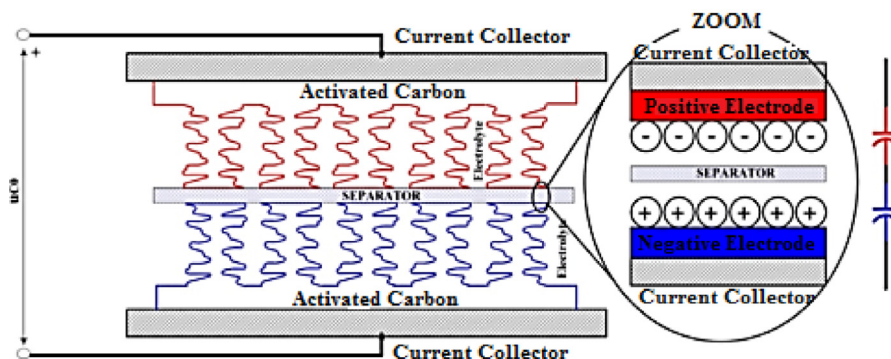


Fig. 7. Supercapacitor cross-section.

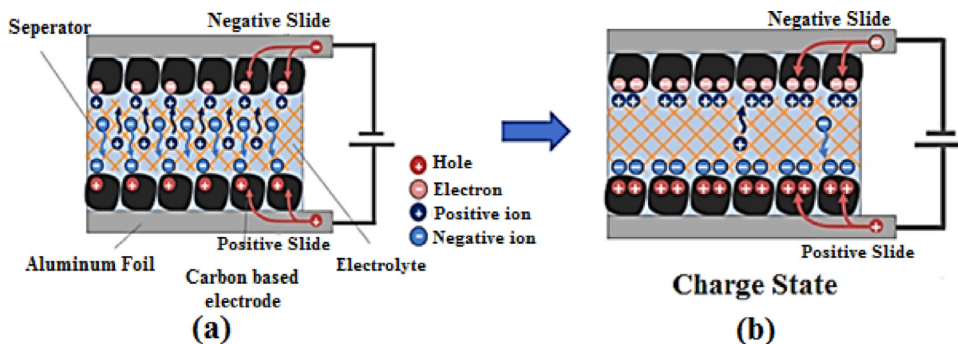


Fig. 8. a) Idle state of supercapacitors, b) Charge state of supercapacitors.

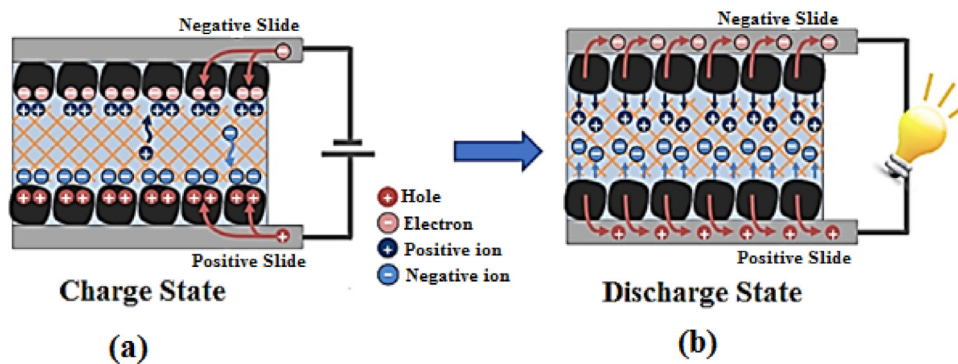


Fig. 9. a) Charge state of supercapacitors, b) Discharge state of supercapacitors.

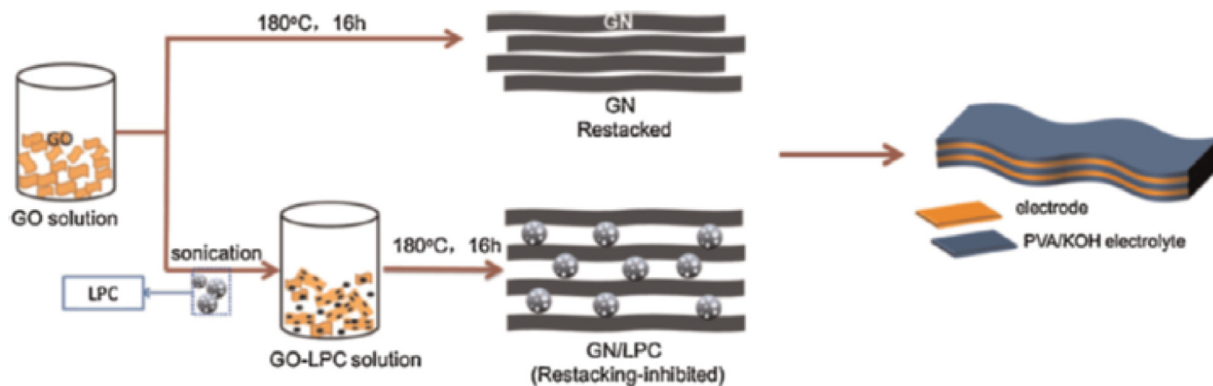


Fig. 10. Schematic illustration of GN aerogel and LGN / PC aerogel and all solid-state supercapacitors.

Aken, K.L.V. et al. produced single walled carbon nanotube aerogels (SWCNT) by drying at critical point. The results indicated that SWCNT aerogels showed an impressive performance in high charges and discharges along with over 10,000 cycles of capacitive performance

because of improved electronic and ionic conductivity of [56].

Yu, Z. et al. produced asymmetric supercapacitors by inserting palladium nanoparticles into the three-dimensional network of graphene oxide. With this doping, the electrical resistance is reduced. P-GA

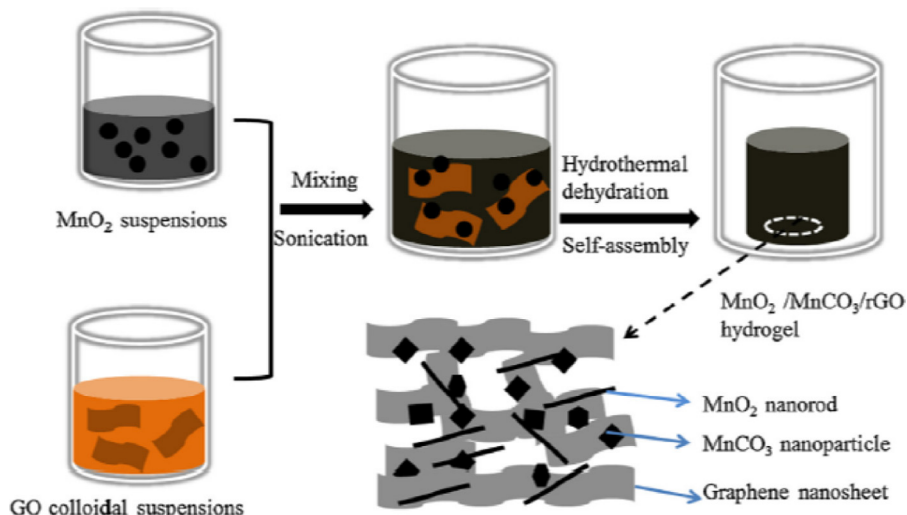


Fig. 11. Illustration of the production process of MnO₂/MnCO₃/rGO hydrogels.

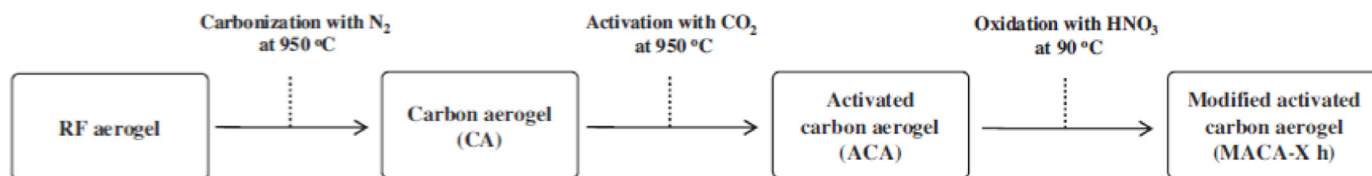


Fig. 12. Procedures for the preparation of modified activated carbon aerogel.

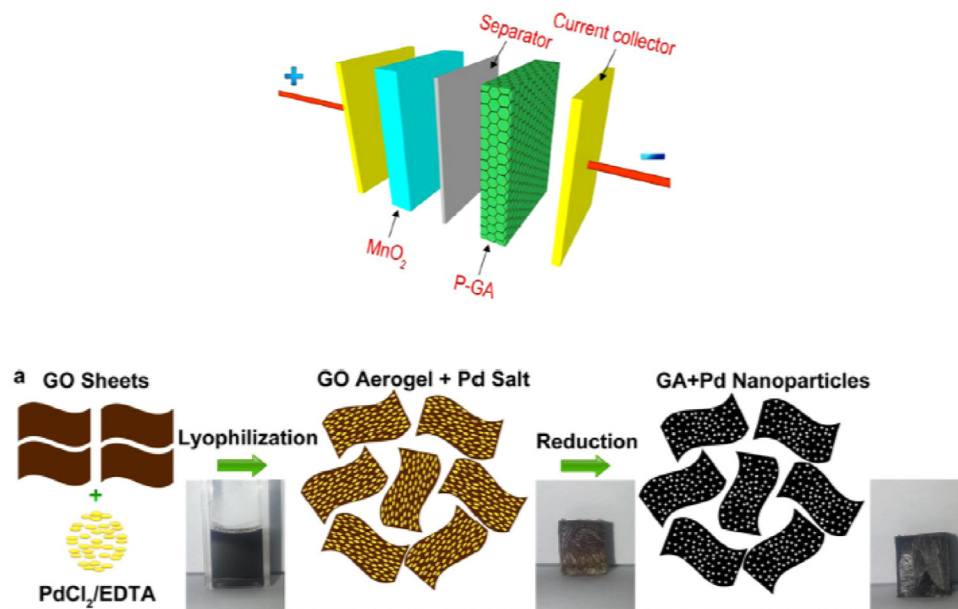


Fig. 13. Schematic illustration of the composed structure of an ASC (based on P-GA as anode and MnO₂ as cathode) and the production process of P-GA.

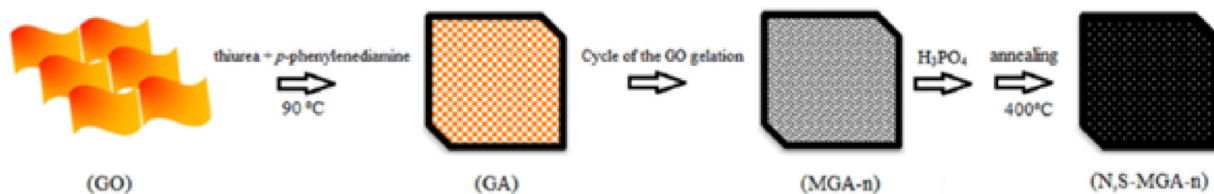


Fig. 14. Procedure for the synthesis of N, S-MGA.

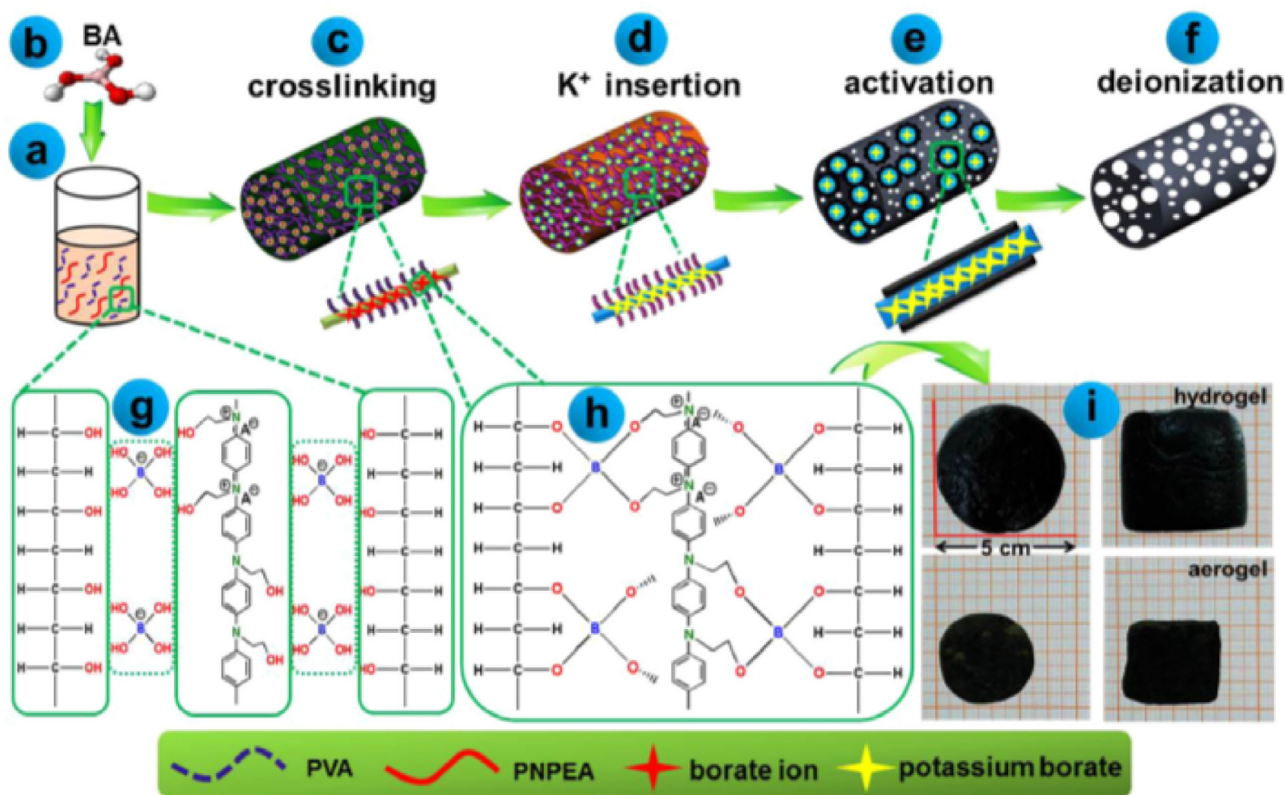


Fig. 15. Schematic self-molded production strategy of aerogels a) Homogeneous mixture of PVA and PEA, b) BA molecule, c) aged hydrogel work, d) carbon aerogel after K insertion, e) carbon KOH, f) further etched aerogel as synthesized 3D hierarchical networks, g) crosslinking process in the hydroxyl group between PVA, PEA and borate ion, h) PVA-borate-PNPEA group, i) digital image hydrogel and aerogel.

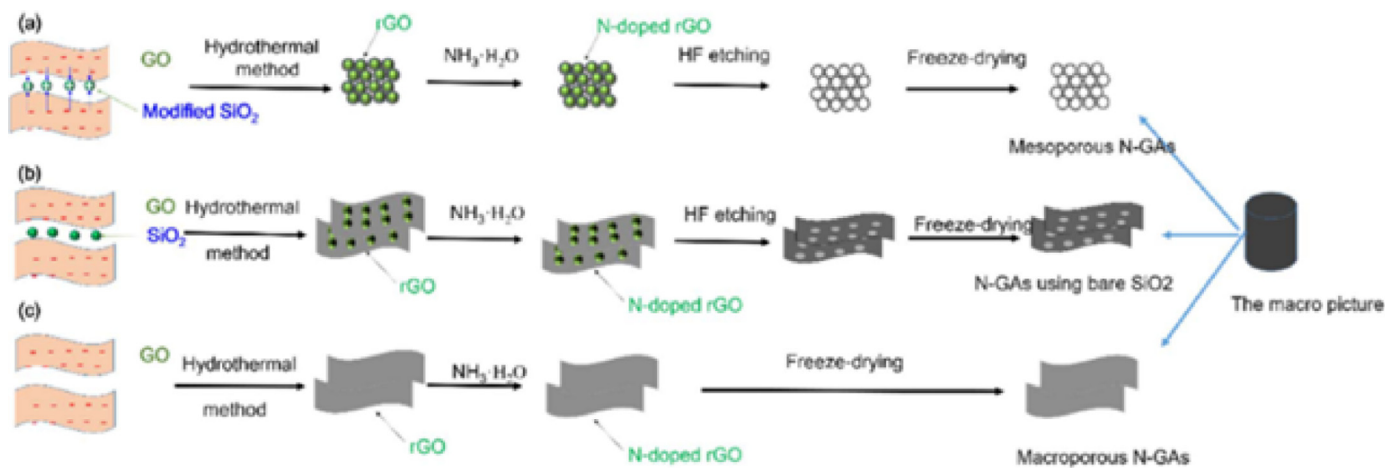


Fig. 16. Schematic diagram of the preparation of Mesoporous N-Gas.

based electrodes exhibited high specific capacitance (175.8 Fg^{-1} at 5 mVs^{-1}) (in Fig. 13). They showed rapid charge, discharge capacity, excellent cycle stability (89.6% after 3000 cycles) and high energy (average 13.9 Whkg^{-1}) and power densities (1 and 13.3 kWkg^{-1}) [57].

Tingting, Y. et al. reported for the first time the synthesis of multiple graphene aerogel (N, S-MGA) with nitrogen and sulfur functionality by simple multiple gel method (in Fig. 14). It was found that the N, S-MGA that they have prepared showed higher density and electrical conductivity than classical graphene aerogels. N, S-MGA electrode provides high specific capacitance (486.8 Fg^{-1} at 1 Ag^{-1} current density) and speed capacity (261.8 Fg^{-1} at 20 Ag^{-1} current density). Specific capacitance is 4929.4 Fg^{-1} at 2 Ag^{-1} current density, in the electrolyte of 1 M KOH mixed with $1 \text{ M K}_3\text{Fe}(\text{CN})_6$. Capacitance retention was above

98.7% after 5000 continuous charge/ discharge cycles and provided good long-term cycle stability. The energy density reaches 686.7 Wkg^{-1} at 1020 Whkg^{-1} power density and 316.6 Wkg^{-1} at 117.6 Whkg^{-1} power density [58].

Wei, X. et al. prepared three-dimensional carbon aerogels with both N-phenyl ethanol amine containing polyvinyl alcohol and nitrogen, and nitrogen sources and boric acid (in Fig. 15). It showed a high surface area up to $2016 \text{ m}^2\text{g}^{-1}$ with a pore volume of $1179 \text{ cm}^3\text{g}^{-1}$. In the three-electrode measuring system, it showed 467 Fg^{-1} high specific capacitance and a significant cycle performance of 85.7% and 90.9%, at 20 Ag^{-1} and 30 Ag^{-1} over 10,000 cycles. It also provided an energy density of 22.75 Whkg^{-1} [59].

Yuan, W. et al. have produced nitrogen-supplemented graphene

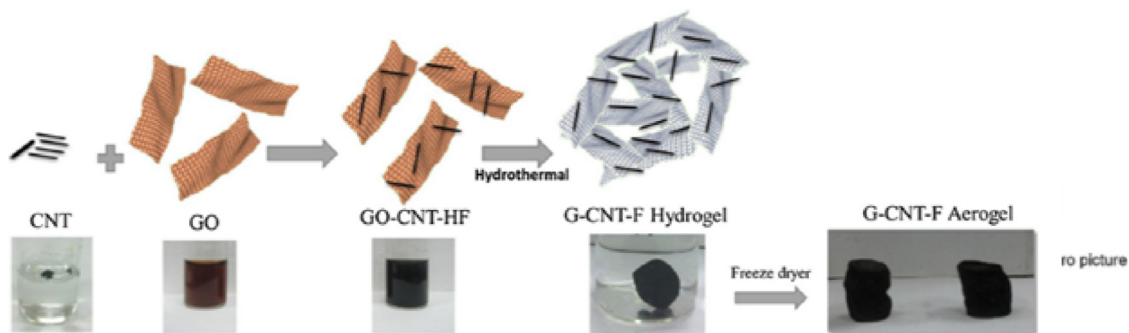


Fig. 17. Preparation of graphene-carbon nanotube composite aerogels.



Fig. 18. Production process of GR-CNTs and Pt / GR-CNTs.

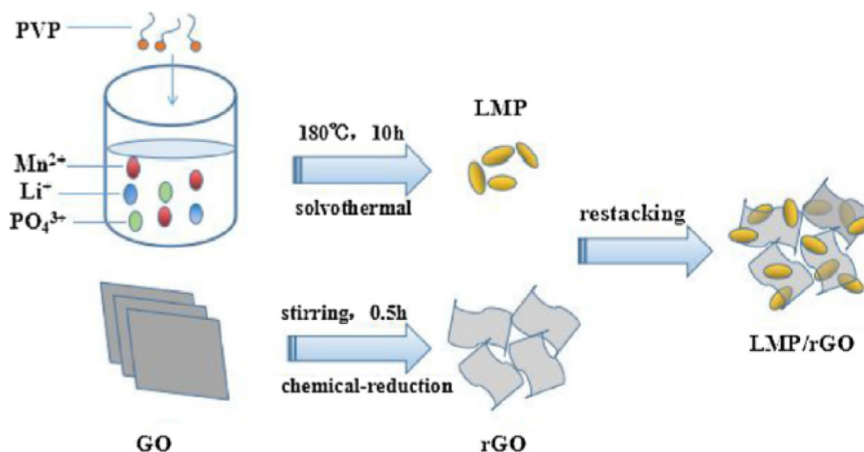


Fig. 19. Schematic illustration of the preparation process of LMP / rGO aerogels.

Table 1
Graphene / graphene oxide aerogels.

Advantages	Disadvantages
Have large surface area Their properties can be improved by connecting functional groups Suitable for the production of supercapacitors with metals A high amount of electrical energy can be stored with metals.	Their production is costly Production processes take a long time. They are fragile and brittle Improvements are required to be able to use them in today's technology.

aerogel using SiO₂ nanoparticles via electrostatic method, which is a new method. Since electrostatic attraction provides a strong interaction between GO and SiO₂ nanoparticles, it was found that SiO₂ templates significantly reduce the number of macro pores in the GAs after HF erosion, highly increasing the number of mesopores (in Fig. 16). As a result of the measurements, a specific capacitance of 203 Fg⁻¹ was achieved at 1 A⁻¹ current density and only 8.95% reduction occurred in the capacitance, at the high current density of 20 Ag⁻¹ [60].

Jokar, E. et al. have improved the conductivity of graphene aerogels produced in two-stage by means of the CNT used as a spacer between the graphene layers and the fluoride doping of the graphene. They examined the effect of fluorene doping on graphene CNT composite (in

Fig. 17). The specific capacitance showed a 78% decrease when the discharge current increased from 2 to 40 mA, a loss of 63.8% and 33.3% was observed on the capacitance of G-CNT and G-CNT F electrodes respectively [61].

Zhou, Y. et al., produced three-dimensional GR-CNT aerogels using graphene oxide and oxidized carbon as precursor, then impregnating with polyvinyl alcohol (pressurized process to remove gaps) and freeze drying (in Fig. 18). A specific capacity of about 375 Fg⁻¹ was obtained from GR-CNT aerogel electrode, in 6 M KOH solution. 88% and 94.8% efficiency were achieved after 5000 cycles. In this study, it was observed that the use of PVA was of great importance in preventing the deformation of GR-CNTs during freezing [62].

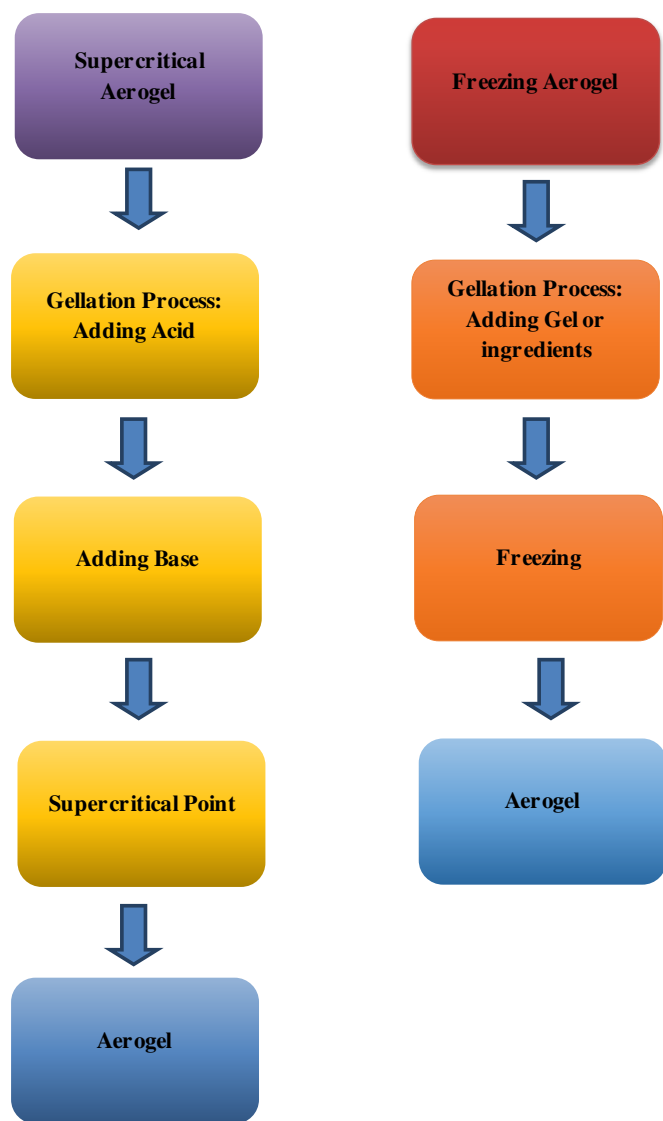


Fig. 20. Progress of Supercritical Aerogels and Freezing Aerogels.

Ghosh, K. et al. have prepared a PANI/(MnO₂ RGO)/PANI flexible asymmetric supercapacitor by using PVA / KOH gel electrolyte as negative electrode material and MoO₃/GF as positive electrode material. At this stage, three-dimensional MnO₂ RGO porous film was produced by vacuum filtration of MnO₂ and GO and then by hydrothermal chemical reduction, thereafter PANI nanofibers were inserted on the hybrid film and three-dimensional PANI / (MnO₂ RGO) / PANI film was obtained. As a result of the electrochemical measurements, a power density of 0.838 kW kg⁻¹ and a high energy density of 51.91 Whkg⁻¹ were observed [63].

Xu, Y. et al. produced oxidation-modified carbon aerogels (OM-CA) from carbon aerogel powders oxidized through Hummers method. To investigate the effect of oxygen groups located at the surface on surface area and electrochemical performance, sulfuric acid stoichiometry was performed. When the amount of sulfuric acid was 40% by weight, the doping manganese content was 0.9 mol%, and the specific surface area of OM-CA was 450 m²g⁻¹ and the specific capacitance was calculated to be 151 Fg⁻¹ at 0.5 Ag⁻¹ current density [64].

Yang, X. et al. used to carbon fiber aerogel (CFA). A specific capacitance of 381 Fg⁻¹ was achieved at a high scanning speed of 200 mV/s. At the same time, it was observed that the material had a great flexibility potential of 86% at a pressure of 23 kPa [65].

Xu, L. et al. Prepared LiMnPO₄/reduced graphene oxide aerogel

(LMP/rGO). They followed polyvinyl pyrrolidone-supported solvothermal route to obtain the LiMnPO₄ nanoparticle (in Fig. 19). They prepared the LMP/rGO aerogel using restacking method. For the best LMP/rGO (with 27.3% rGO), a specific capacitance of 464.5 Cg⁻¹ was obtained at 0.5 Ag⁻¹ current density [66].

Wang, H. et al., synthesized Fe₂O₃@multiple graphene aerogels (F-Fe₂O₃ @ MGA). F-Fe₂O₃ was hybridized with graphene by multiple gelation method, the prepared F-Fe₂O₃ @ MGA provided three-dimensional structure. Synthesized F-Fe₂O₃ @ MGA showed high electron/ion conductivity and good structural stability. As a result of the electrochemical measurements made for the composite electrode produced for supercapacitors, a specific capacitance of 1119 Fg⁻¹ was obtained at 1 Ag⁻¹ current density, and specific capacitances of 492 and 630 Fg⁻¹ at 10 Ag⁻¹ current density. Moreover, an energy density of 800 Whkg⁻¹ was detected at 8000 Whkg⁻¹ power density and 95.3 Whkg⁻¹ energy density at 45 Whkg⁻¹ power density [67].

Wang, B. et al. produced macro, meso and micro porous carbon aerogels (CAs) using renewable natural alginate. Specific capacitance values of APCAs (800) calculated according to charge times were measured to be 188, 176, 160, 150, 139, 128 and 122 Fg⁻¹ at 1, 2, 5, 10, 20, 50 and 100 Ag⁻¹ current density [68].

Jayaseelana, S. S. et al., produced mesoporous 3D NiCo₂O₄/MWCNT nanocomposite aerogels by supercritical CO₂ drying through sol-gel method. NiCo₂O₄/MWCNT nanocomposite aerogels, whose MWCNT ~% 2,1 wt, have been found to reach a specific capacity of 1010 Fg⁻¹ at 0.1 Ag⁻¹ discharge current density. Solid-state is applied to asymmetric supercapacitors and they exhibited a good field stability and higher field capacitance values (471,8 mFcm⁻²) at 5 mAcm⁻² current density [69].

Li, F. et al., freeze-dried carbon aerogel microsphere (CAM) prepared by sol-gel, and the aerogels were heat treated at 600, 800, 1000, 1200, 1400 and 1600 °C. It was found that the CAMs carbonized at 1000 °C have the highest SSA (1454 m²/g), large meso-porous content (20%) and appropriate conductivity (71 Scm⁻¹). A high energy density (38.4 Whkg⁻¹) was achieved at 0.17 kWkg⁻¹ power density. Even at a high-power density of 10.2 kWkg⁻¹, an energy density of 25.5 Whkg⁻¹ and a good cycling capability of 84% were observed after 10,000 rpm [70].

Zeng, F. Y. et al. investigated the contribution of nitrogen atoms to carbon aerogels. Nitrogen doped carbon aerogels were prepared by the polymerization of pyrrole and formaldehyde monomers under hypersaline conditions, followed by carbonization at different temperatures (800 and 900 °C). As a result of electrochemical measurements, CV curves computed specific capacitance at 100 mV s⁻¹ scanning rate as 140 Fg⁻¹ for NCA-800 and as 115 Fg⁻¹ for NCA-900 [71].

6. Conclusion

According to the literature sources cited above, graphene / graphene oxide aerogels have both advantages and disadvantages. Table 1 also displays the advantages and disadvantages.

As a result, regarding the aerogels which have high potential in many areas, their production processes and properties need to be improved not only academically but also for the sake of potential applicability. Because they can still be produced in very low amounts in the laboratory. This is one of the factors limiting their usage in today's technology. At the same time, the production cost is still high. But researchers continue to conduct many studies in this area. If these problems can be eliminated, it is thought that they will lead to great technological developments especially in the field of energy.

If we want to produce devices that can store higher energy, we certainly need aerogels. Because, as mentioned earlier, bulk materials (even reduced graphene oxide) do not have a surface area as large as that of aerogels. Graphene oxide having a surface area of 2630 m²g⁻¹ can be improved by at least two or three times in the aerogel form. As we mentioned at the end of Chapter 4, it was found that the amount of

stored charge in the supercapacitors is excessively increased, with the increase of the roughness and surface area of the electrodes.

Reduced graphene oxide can be produced by chemists more easily and cost-effectively than aerogel graphene oxide. But we are sure that chemists will develop suitable methods for the production of graphene oxide aerogel in the future. A typical example is the aerogels produced by cooling the gelled materials below $-78\text{ }^{\circ}\text{C}$ by a freeze dryer. This method can be found in newly published papers as freezing aerogel production. Figure 20 schematically illustrates the production process of aerogels produced by supercritical method and freezing.

As can be seen, it is possible to produce aerogel with at least one step less process and less cost.

Therefore, in future studies focusing on RGO/Carbon nanotube aerogels, RGO/Fullerene aerogels, RGO/C60 aerogels and also with the metal oxides to be added to them as impurities, it is possible to produce supercapacitors which can store several thousand Farad charge per gram.

Declaration of Competing Interest

“I, the Corresponding Author, declare that this manuscript is original, has not been published before and is not currently being considered for publication elsewhere.

I would like to draw the attention of the Editor to the following publications of one or more of us that refer to aspects of the manuscript presently being submitted.

We can confirm that the manuscript has been read and approved by all named authors and that there are no other persons who satisfied the criteria for authorship but are not listed. I further confirm that the order of authors listed in the manuscript has been approved by all of us.

And also we have no any conflict interest.

This study have no any source(s) of support in the form of grants, bursaries, free use of equipment, drugs or any other benefits.

We understand that the Corresponding Author is the sole contact for the Editorial process and is responsible for communicating with the other authors about progress, submissions of revisions and final approval of proofs.

References

- J.R. Miller, P. Simon, Electrochemical capacitors for energy management, *Science* 321 (2008) 651–652.
- Z.S. Wu, A. Winter, L. Chen, Y. Sun, A. Turchanin, X. Feng, K. Müllen, Three dimensional nitrogen and boron co-doped graphene for high-performance all solid-state supercapacitors, *Adv. Mater.* 24 (2012) 5130.
- G.M. Wang, H.Y. Wang, X.H. Lu, Y.C. Ling, M.H. Yu, T. Zhai, Y.X. Tong, Y. Li, Solid state supercapacitor based on activated carbon cloths exhibits excellent rate capability, *Adv. Mater.* 26 (2014) 2676.
- K. Gong, F. Du, Z. Xia, M. Durstock, L. Dai, Nitrogen-Doped carbon nanotube arrays with high electrocatalytic activity for oxygen reduction, *Science* 323 (2009) 760–764.
- L.T. Song, Z.Y. Wu, H.W. Liang, F. Zhou, Z.Y. Yu, L. Xu, Z. Pan, S.H. Yu, Macroscopic-scale synthesis of nitrogen-doped carbon nanofiber aerogels by template-directed hydrothermal carbonization of nitrogen-containing carbohydrates, *Nano Energy* 19 (2016) 117–127.
- X. Wei, X. Jiang, J. Wei, S. Gao, Functional groups and pore size distribution do matter to hierarchically porous carbons as high-rate-performance supercapacitors, *Chem. Mater.* 28 (2016) 445–458.
- J. Biener, M. Stadermann, M. Suss, M.A. Worsley, M.M. Biener, K.A. Rose, T.F. Baumann, Advanced carbon aerogels for energy applications, *Energy Environ. Sci.* 4 (2011) 656–667.
- H. Gao, Y.J. Ting, N.P. Kherani, K. Lian, Ultra-high-rate all-solid pseudocapacitive electrochemical capacitors, *J. Power Sources* 222 (2013) 301–304.
- B. Hui, Y. Zhang, L. Ye, Preparation of PVA hydrogel beads and adsorption mechanism for advanced phosphate removal, *Chem. Eng. J.* 235 (2014) 207–214.
- C. Liu, G. Han, Y. Chang, Y. Xiao, M. Li, W. Zhou, Monolithic porous carbon derived from polyvinyl alcohol for electrochemical double layer capacitors, *Electrochim. Acta* 188 (2016) 175–183.
- C.D. Blasi, C. Branca, A. Galgano, Thermal and catalytic decomposition of wood impregnated with sulfur and phosphorus-containing ammonium salts, *Polym. Degrad. Stab.* 93 (2008) 335–346.
- W.C. Li, A.H. Lu, S.C. Guo, Characterization of the microstructures of organic and carbon aerogels based upon mixed cresol-formaldehyde, *Carbon N Y* 39 (2001) 1989–1994.
- W. Deng, Y. Zhang, Y. Tan, M. Ma, Three-dimensional nitrogen-doped graphene derived from poly-o-phenylenediamine for high-performance supercapacitors, *J. Electroanal. Chem.* 787 (2017) 103–109.
- C. Xu, F. Kang, B. Li, H. Du, Recent progress on manganese dioxide based supercapacitors, *J. Mater. Res.* 25 (2010) 1421–1432.
- Y. Yoon, W. Cho, J. Lim, D. Choi, Solid-state thin-film supercapacitor with ruthenium oxide and solid electrolyte thin films, *J. Power Sources* 101 (2001) 126–129.
- Z. Tang, C. Tang, H. Gong, A high energy density asymmetric supercapacitor from nano-architected ni (OH) 2/Carbon nanotube electrodes, *Adv. Funct. Mater.* 22 (2012) 1272–1278.
- Z.C. Yang, C.H. Tang, Y. Zhang, H. Gong, X. Li, J. Wang, Cobalt monoxide-doped porous graphitic carbon microspheres for supercapacitor application, *Sci. Rep.* 3 (2013) 2925.
- S. Nardecchia, D. Carriazo, M.L. Ferrer, M.C. Gutiérrez, F. del Monte, Three dimensional macroporous architectures and aerogels built of carbon nanotubes and/or graphene: synthesis and applications, *Chem. Soc. Rev.* 42 (2013) 794–830.
- S. Hu, S. Zhang, N. Pan, Y.L. Hsieh, High energy density supercapacitors from lignin derived submicron activated carbon fibers in aqueous electrolytes, *J. Power Source* 270 (2014) 106–112.
- B. Xu, S. Yue, Z. Sui, X. Zhang, S. Hou, G. Cao, Y. Yang, What is the choice for supercapacitors: graphene or graphene oxide? *Energy Environ. Sci.* 4 (2011) 2826–2830.
- H. Kim, A.A. Abdala, C.W. Macosko, Graphene/Polymer nanocomposites, *Macromolecules* 43 (2010) 6515–6530.
- D.C. Marcano, D.V. Kosynkin, J.M. Berlin, A. Sinitskii, Z. Sun, A. Slesarev, L.B. Alemany, W. Lu, J.M. Tour, Improved synthesis of graphene oxide, *Amercan Chem. Soc. ACS Nano* 4 (8) (2010) 4806–4814.
- H. Ke, Z. Pang, Y. Xu, X. Chen, J. Fu, Y. Cai, F. Huang, Q. Wei, Graphene oxide improved thermal and mechanical properties of electrospun methy stearate/polyacrylonitrile from-stable phase cahnge composite nanofibers, *J. Therm. Anal. Calorim.* 117 (1) (2014) 109–122.
- P. Wagh, R. Begag, G. Pajonk, A.V. Rao, D. Haranath, Comparison of some physical properties of silica aerogel monoliths synthesized by different precursors, *Mater. Chem. Phys.* 57 (1999) 214–218.
- A. Du, B. Zhou, Z. Zhang, J. Shen, A special material or a new state of matter: a review and reconsideration of the aerogel, *Materials* 6 (2013) 941–968.
- Y. Zhu, S. Murali, W. Cai, X. Li, J.W. Suk, J.R. Potts, R.S. Ruoff, Graphene and graphene oxide: synthesis, properties, and applications, *Adv. Mater.* 22 (2010) 3906–3924.
- M.A. Aegerter, N. Leventis, M.M. Koebel, *Aerogels Handbook*, Springer, New York, NY, USA, 2011.
- B. Mena, F. Mena, C. Aiolfi-Guimaraes, O. Sharts, Silica-based nanoporous sol-gel glasses: from bioencapsulation to protein folding studies”, *Int. J. Nanotechnol.* 7 (2010) 1–45.
- L.H. Gan, T.Y. Yue, L.W. Chen, G.M. Li, B. Zhou, Preparation and characterization of beta-FeOOH aerogels, *Acta Phys. Chim. Sin.* 13 (1997) 48–51.
- A.E. Gash, T.M. Tillotson, J.H. Satcher Jr., J.F. Poco, L.W. Hrubesh, R.L. Simpson, Use of epoxides in the sol-gel synthesis of porous iron (III) oxide monoliths from Fe (III) salts, *Chem. Mater.* 13 (2001) 999–1007.
- A.E. Gash, J.H. Satcher, R.L. Simpson, Monolithic nickel (II)-based aerogels using an organic epoxide: the importance of the counterion, *J. Non-Cryst. Solids* 350 (2004) 145–151.
- Y.T. Bi, H.B. Ren, B.W. Chen, L. Zhang, Synthesis and characterization of nickel-based monolithic aerogel via sol-gel method, *Adv. Mater. Res.* 335–336 (2011) 368–371.
- T.F. Baumann, A.E. Gash, S.C. Chinn, A.M. Sawvel, R.S. Maxwell, J.H. Satcher, Synthesis of high-surface-area alumina aerogels without the use of alkoxide precursors, *Chem. Mater.* 17 (2005) 395–401.
- T.F. Baumann, S.O. Kucheyev, A.E. Gash, J.H. Satcher, Facile synthesis of a crystalline, high-surface-area SNO2 aerogel, *Adv. Mater.* 17 (2005) 1546–1548.
- S.O. Kucheyev, B. Sadigh, T.F. Baumann, Y.M. Wang, T.E. Felter, T. Van Buuren, A.E. Gash, J.H. Satcher, A.V. Hamza, Electronic structure of chromia aerogels from soft X-ray absorption spectroscopy, *J. Appl. Phys.* 101 (2007) 315 1–124 315:8.
- A. Du, B. Zhou, J. Shen, J.Y. Gui, Y.H. Zhong, C.Z. Liu, Z.H. Zhang, G.M. Wu, A versatile sol-gel route to monolithic oxidic gels via polyacrylic acid template, *New J. Chem.* 35 (2011) 1096–1102.
- H.B. Ren, L. Zhang, C.W. Shang, X. Wang, Y.T. Bi, Synthesis of a low-density tantalum oxide tile-like aerogel monolithic, *J. Sol-Gel Sci. Technol.* 53 (2010) 307–311.
- C. Frederick, A. Forsman, J. Hund, S. Eddinger, Fabrication of Ta2O5 aerogel targets for radiation transport experiments using thin film fabrication and laser processing, *Fusion Sci. Technol.* 55 (2009) 499–504.
- L. Zhang, H.B. Ren, X. Wang, Y.T. Bi, Y.H. Fan, Characterization of monolithic tantalum oxide aerogels using epichlorohydrin as gel initiator, *Rare Met. Mater. Eng.* 39 (2010) 154–156.
- H.C. Chien, W.Y. Cheng, Y.H. Wang, S.Y. Lu, Ultrahigh specific capacitances for supercapacitors achieved by nickel cobaltite/carbon aerogel composites, *Adv. Funct. Mater.* 22 (2012) 5038–5043.
- Y.H. Lin, T.Y. Wei, H.C. Chien, S.Y. Lu, Manganese oxide/carbon aerogel composite: an outstanding supercapacitor electrode material, *Adv. Energy Mater.* 1 (2011) 901–907.
- T.Y. Wei, C.H. Chen, H.C. Chien, S.Y. Lu, C.C. Hu, A cost-effective supercapacitor material of ultrahigh specific capacitances: spinel nickel cobaltite aerogels from an epoxide-driven sol-gel process, *Adv. Mater.* 22 (2010) 347–351.
- C.A. Back, J.D. Bauer, J.H. Hammer, B.F. Lasinski, R.E. Turner, P.W. Rambo,

- O.L. Landen, L.J. Suter, M.D. Rosen, W.W. Hsing, Diffusive, supersonic X-ray transport in radiatively heated foam cylinders, *Phys. Plasmas* 7 (2000) 2126–2134.
- [44] C.A. Back, J.F. Seely, J.L. Weaver, U. Feldman, R. Tommasini, S.G. Glendinning, H.K. Chung, M. Rosen, R.W. Lee, H.A. Scott, Underdense radiation sources: moving towards longer wavelengths, *J. Phys. IV* 133 (2006) 1173–1175.
- [45] K.B. Fournier, J.H. Satcher, M.J. May, J.F. Poco, C.M. Sorce, J.D. Colvin, S.B. Hansen, S.A. Mac Laren, S.J. Moon, J.F. Davis, Absolute X-ray yields from laser-irradiated germanium-doped low-density aerogels, *Phys. Plasmas* 16 (2009) 0527031–052703:13.
- [46] J.D. Colvin, K.B. Fournier, M.J. May, H.A. Scott, A computational study of X-ray emission from laser-irradiated Ge-doped foams, *Phys. Plasmas* 17 (2010) 0731111–073111:8.
- [47] M. Tanabe, H. Nishimura, N. Ohnishi, K.B. Fournier, S. Fujioka, A. Iwamae, S.B. Hansen, K. Nagai, F. Girard, M. Primout, B. Villette, D. Brebion, K. Mima, Characterization of heat-wave propagation through laser-driven Ti-doped underdense plasma, *High Energy Density Phys* 6 (2010) 89–94.
- [48] F. Girard, M. Primout, B. Villette, D. Brebion, H. Nishimura, K.B. Fournier, Experimental X-ray characterization of Gekko-XII laser propagation through very low-density aerogels (2–5 mg/cc) creating multi-keV photons from a titanium solid foil, *High Energy Density Phys* 7 (2011) 285–287.
- [49] R.A. Ganeev, Generation of harmonics of laser radiation in plasmas, *Laser Phys. Lett.* 9 (2012) 175–194.
- [50] F. Perez, J.J. Kay, J.R. Patterson, J. Kane, B. Villette, F. Girard, C. Reverdin, M. May, J. Emig, C. Sorce, Efficient laser-induced 6–8 keV X-ray production from iron oxide aerogel and foil-lined cavity target, *Phys. Plasmas* 19 (2012) 0831011–083101:10.
- [51] R. Pekala, Organic aerogels from the polycondensation of resorcinol with formaldehyd, *J. Mater. Sci.* 24 (1989) 3221–3227.
- [52] Z. Song, W. Liu, P. Xiao, Z. Zhao, G. Liu, J. Qiu, Nano-iron oxide (Fe₂O₃)/three-dimensional graphene aerogel composite as supercapacitor electrode materials with extremely wide working potential window, *Mater Lett* 145 (2015) 44–47.
- [53] T.T. Chen, W.L. Song, L.Z. Fan, Engineering graphene aerogels with porous carbon of large surface area for flexible all-solid-state supercapacitors, *Electrochim. Acta* 165 (2015) 92–97.
- [54] Y. Liu, D. He, H. Wu, J. Duan, Y. Zhang, Hydrothermal self-assembly of manganese dioxide/manganese carbonate/reduced graphene oxide aerogel for asymmetric supercapacitors, *Electrochim. Acta* 164 (2015) 154–162.
- [55] E.J. Lee, Y.J. Lee, J.K. Kim, M. Lee, J. Yi, J.R. Yoon, J.C. Song, I.K. Song, Oxygen group-containing activated carbon aerogel as an electrode material for supercapacitor, *Mater. Res. Bull.* 70 (2015) 209–214.
- [56] K.L.V. Akena, C.R. Pérez, Y. Oh, M. Beidaghi, Y.J. Jeong, M.F. Islam, Y. Gogotsi, High rate capacitive performance of single-walled carbon nanotube aerogels, *Nano Energy* 15 (2015) 662–669.
- [57] Z. Yu, M.M. Innis, J. Calderon, S. Seal, L. Zhain, J. Thomas, Functionalized graphene aerogel composites for high-performance asymmetric supercapacitor, *Nano Energy* 11 (2015) 611–620.
- [58] Y. Tingting, L. Ruiyi, L. Xiaohuan, L. Zaijun, G. Zhiguo, W. Guangli, L. Junkang, Nitrogen and sulphur-functionalized multiple graphene aerogel for supercapacitors with excellent electrochemical performance, *Electrochim. Acta* 187 (2016) 143–152.
- [59] X. Wei, S. Wan, S. Gao, Self-assembly-template engineering nitrogen-doped carbon aerogels for high-rate supercapacitors, *Nano Energy* 28 (2016) 206–215.
- [60] W. Yuan, L. Cheng, Y. Zhang, Y. Li, X. Guo, H. Wu, L. Zheng, Mesoporous nitrogen-doped graphene aerogels with enhanced rate capability towards high performance supercapacitors, *Ceram. Int.* 43 (2017) 11563–11568.
- [61] E. Jökar, S. Shahrokhian, A. Irajizad, E. Asadian, H. Hosseini, An efficient two-step approach for improvement of graphene aerogel characteristics in preparation of supercapacitor electrodes, *J. Energy Storage* 17 (2018) 465–473.
- [62] Y. Zhou, X.C. Hu, S. Guo, C. Yu, S. Zhong, X. Liu, Multi-functional graphene/carbon nanotube aerogels for its applications in supercapacitor and direct methanol fuel cell, *Electrochim. Acta* 264 (2018) 12–19.
- [63] K. Ghosh, C.Y. Yue, Development of 3D MoO₃ graphene aerogel and sandwich-type polyaniline decorated porous MnO₂ graphene hybrid film based high performance all-solid-state asymmetric supercapacitors, *Electrochim. Acta* 276 (2018) 47–63.
- [64] Y. Xu, B. Ren, S. Wang, L. Zhang, Z. Liu, Carbon aerogel-based supercapacitors modified by hummers oxidation method, *J. Colloid Interface. Sci.* 527 (2018) 25–32.
- [65] X. Yang, B. Fei, J. Ma, X. Liu, S. Yang, G. Tian, Z. Jiang, Porous nanoplatelets wrapped carbon aerogels by pyrolysis of regenerated bamboo cellulose aerogels as supercapacitor electrodes, *Carbohydr. Polym* 180 (2018) 385–392.
- [66] L. Xu, S. Wang, X. Zhang, T. He, F. Lu, H. Li, J. Ye, A facile method of preparing LiMnPO₄/reduced graphene oxide aerogel as cathodic material for aqueous lithium-ion hybrid supercapacitors, *Appl. Surf. Sci.* 428 (2018) 977–985.
- [67] H. Wang, R. Li, M. Li, Z. Li, Flower-like Fe₂O₃@multiple graphene aerogel for high-performance supercapacitors, *J. Alloys Compd.* 742 (2018) 759–768.
- [68] B. Wang, D. Li, M. Tang, H. Ma, Y. Gui, X. Tian, F. Quan, X. Song, Y. Xia, Alginate-based hierarchical porous carbon aerogel for high-performance supercapacitors, *J. Alloys Compd.* 749 (2018) 517–522.
- [69] S.S. Jayaseelan, S. Radhakrishnan, B. Saravanakumar, M.K. Seo, M.S. Khil, H.Y. Kim, B.S. Kim, Mesoporous 3D NiCo₂O₄/MWCNT nanocomposite aerogels prepared by a supercritical CO₂ drying method for high performance hybrid supercapacitor electrodes, *Colloid. Surf. A* 538 (2018) 451–459.
- [70] F. Li, L. Xie, G. Sun, F. Su, Q. Kong, Y. Cao, X. Guo, C. Chen, Structural evolution of carbon aerogel microspheres by thermal treatment for high-power supercapacitors, *J. Energy Chem.* 27 (2018) 439–446.
- [71] F.Y. Zeng, Z.Y. Sui, S. Liu, H.P. Liang, H.H. Zhan, B.H. Han, Nitrogen-doped carbon aerogels with high surface area for supercapacitors and gas adsorption, *Mater. Today Commun.* 16 (2018) 1–7.